Social Network Optimization Based Procedure for Beam-Scanning Reflectarray Antenna Design

IEEE Open Journal of
Antennas and Propagation

Received 6 August 2020; revised 1 September 2020; accepted 1 September 2020. Date of publication 8 September 2020; date of current version 5 October 2020.

Digital Object Identifier 10.1109/OJAP.2020.3022935

Social Network Optimization Based Procedure for Beam-Scanning Reflectarray Antenna Design

ALESSANDRO NICCOLAI [1] (Member, IEEE), MICHELE BECCARIA [2] (Member, IEEE), RICCARDO E. ZICH [1] (Member, IEEE), ANDREA MASSACCESI [2] (Member, IEEE), AND PAOLA PIRINOLI [2,3] (Member, IEEE)

[1] Dipartimento di Energia, Politecnico di Milano, 20156 Milan, Italy

[2] Dipartimento di Elettronica e Telecomunicazioni, Politecnico di Torino, 10129 Turin, Italy

[3] Istituto di Elettronica e di Ingegneria dell'Informazione e delle Telecomunicazioni, National Research Council of Italy, 10129 Turin, Italy

CORRESPONDING AUTHOR: A. NICCOLAI (e-mail: alessandro.niccolai@polimi.it)

ABSTRACT Evolutionary algorithms can be successfully exploited for carrying on an effective design of beam-scanning passive reflectarrays, even if the problem is highly non-linear and multimodal. In this article, the Social Network Optimization (SNO) algorithm has been used for assessing an effective design procedure of a beam-scanning passive reflectarray (RA). For exploiting at most the optimization capabilities of SNO, the entire optimization environment has been deeply analyzed in all its parts. The performance of SNO and the beam-scanning capabilities of the optimized RA have been assessed through the comparison with other well established Evolutionary Algorithms.

INDEX TERMS Social network optimization, beam-scanning reflectarray, optimization environment, evolutionary optimization.

I. INTRODUCTION

In THE past years, Evolutionary Algorithms (EAs) have been successfully applied to antenna problems, thanks to their capability to find optimal solutions in nonlinear and multimodal problems [1], [2]. Among the various EAs, the most used, in particular for the array pattern synthesis, are the Genetic Algorithm (GA) [3], [4], the Differential Evolution (DE) [5] and Particle Swarm Optimization (PSO) [6]. To improve the algorithms performance, especially related to their convergence capability, some hybrid approaches were also proposed: in [7] a technique obtained by hybridizing GA and PSO is presented, while in [8] and [9] the PSO alone or in conjunction with the GA is further hybridized with the Taguchi method. In [10], the genetic algorithm is combined with a local optimization approach, and in [11], [12] the convex programming is used to increase the performance of the single objective or the multi-objective PSO, respectively.

The high efficiency of the EAs for array pattern problems has also been exploited to design reflectarray configurations. Reflectarray antennas (RAs) have established themselves as powerful and efficient high-gain antennas, thanks to their numerous advantages, including the low profile, low cost, good radiation performance and ease of manufacturing [13], [14]. Compared to traditional phased arrays, they exploit the space feeding to avoid the complexity and losses introduced by the feeding networks [15]. The design of a pencil beam RA is typically carried out analytically: the degrees of freedom of each unit cell are fixed to produce the required phase shift on the RA aperture [13], [14]. If more complex radiation patterns, as shaped or contoured beams, are required or if the focus is the steering of the pointing direction, alternative solutions must be exploited, mostly based on the use of an optimization algorithm [14].

Since a reflectarray is generally composed by many elements (even thousands) that all contribute to the generation of the radiation pattern, the optimization algorithm must be computationally efficient to manage a large number of variables. The most used approach to this array synthesis problem is the phase-only method, which involves only the reflection phase of the elements in the optimization process. A well-known local optimization routine that uses the phase-only synthesis is called Intersection Approach (IA) or Alternating Projection Method (APM) [16]–[18]. In this algorithm the solution is iteratively searched between the

intersection of two suitable sets: the set of possible radiation patterns and the set of radiation patterns that satisfy the mask requirements. The efficiency of this technique has been demonstrated by several RA designs with custom radiation patterns, such as contoured beam [19], shaped-beam [20] and asymmetric multibeam [21]. Although the APM is a robust algorithm with a fast convergence, it requires a suitable choice of the first guesses starting points, usually derived by direct design synthesis, since there is a high risk that the algorithm stagnates in a local minimum.

In order to overcome this limitation, global optimizers, as the EAs, can be adopted. The GA has been employed to design a reconfigurable RA with shaped-beam [22] or to determine arbitrarily-shaped conductive elements for microstrip RAs [23]. In [24], a DE-based process has been used to find the positions of square patches on an unequally spaced RA. In [25], a single-feed RA with asymmetric multiple beams has been designed through a PSO-based routine, optimizing only the phase of the RA elements, while, the beam-scanning capabilities of a Ka-band RA have been improved in [26], through a phase-only synthesis that uses a PSO algorithm to flatten the gain in a wide scanning coverage. PSO has been also exploited to enhance the bandwidth of a RA respect to a conventional dual-frequency design, as proposed in [27]. A direct optimization method can also be used to optimize the geometrical parameters of the array cells. Examples on the use of this approach are reported in [28] and [29]: large RAs with contoured beams have been optimized using the spectral domain Method of Moments (MoM), assuming local periodicity and minimax optimization. A generalized version of this procedure has been presented in [30]: the algorithm optimizes arbitrarily shaped elements with irregular orientation and position. These techniques exploit several degrees of freedom to synthesize both co-polar and cross-polar components. However, the computational time increases with the number of optimizing variables. An efficient technique for the optimization of the cross-polarization of dual-polarized RAs has been proposed in [31]: it combines MoM full-wave analysis with local periodicity and optimization processes based on the intersection approach and the Levenberg-Marquardt Algorithm (LMA). Novel techniques exploiting the machine learning algorithm known as Support Vector Machine (SVM) have been recently introduced [32]–[34]: a surrogate model of the RA unit-cell is created using the SVM, achieving accurate results and reduced computational time. In one of the most recent works [35], a System-by-Design strategy for synthesizing RAs has been proposed: it is based on a multiscale task-oriented synthesis approach where the degrees-of-freedom are defined at the microscale in terms of unit-cell descriptors, while the design objectives are defined at the macroscale as constraints on the RA radiation features.

In this article, a novel approach for the synthesis of reflectarrays with improved beam-scanning capabilities is presented. The procedure is based on the use of an innovative and efficient evolutionary algorithm, the Social Network Optimization (SNO), which has already shown extremely promising results dealing with a similarly complex class of problems [36]. The application of a pseudo-stochastic algorithm to the design of a RA is not straightforward [37]: in fact, if the optimization environment is not suitably defined, the RA configuration resulting at the end of the iterative process does not fulfil the hypothesis of quasi-periodicity and therefore its actual behavior strongly differs from the predicted one. On the contrary, when the optimization problem is properly described, the antenna is correctly designed, even if the evaluation of its radiation pattern during the optimization process is done with an approximated approach as the aperture field method [38] adopted here. This is particularly important in order to keep under control the computational time, that otherwise will increase too much, making unfeasible the use of an optimizer for the RA design. For this reason, here a careful analysis of the algorithm parameters have been firstly carried out; then, the optimization environment has been defined: a proper choice of the optimization variables and their representation has been done, as well as of the ratio between the population size and the total number of objective function calls. According to authors' knowledge, results of such an analysis are not yet available in literature, even if they provide useful indication for the application of SNO (and consequently other EAs) to a class of problems like that represented by the beam-scanning RA. Its optimization is intrinsically a multi-objective problem [26]: however, the different objectives have been here merged in a single cost function through a new two-step scalarization procedure, in order to reduce the process computational time. Finally, an additional cost function has been introduced to what generally considered in literature [14], to speed up the SNO convergence and the quality of the obtained solution.

The paper is organized as in the following. In Section II an overview of the SNO is given, and the results of the carried out parametric analysis and of the comparison with other EAs are discussed. In Section III the considered optimization problem is introduced, while in Section IV the features of the optimization environment are established. Finally, in Section V the SNO effectiveness is assessed through its comparison with the results provided by other EAs and the full-wave simulation of the optimized RA.

II. SOCIAL NETWORK OPTIMIZATION

The Social Network Optimization (SNO) is a population-based algorithm that mimics the information sharing process in common online social networks, and therefore its population consists in the social network users that share their ideas and interact online on the social network wall. Figure 1 shows the algorithm logic, where the data structures are represented by rectangles, while the algorithm operators by ovals.

Each user is characterized by its opinion that is shared by means of a post (out of the metaphor, the candidate solution of the optimization problem). The process of creation of a

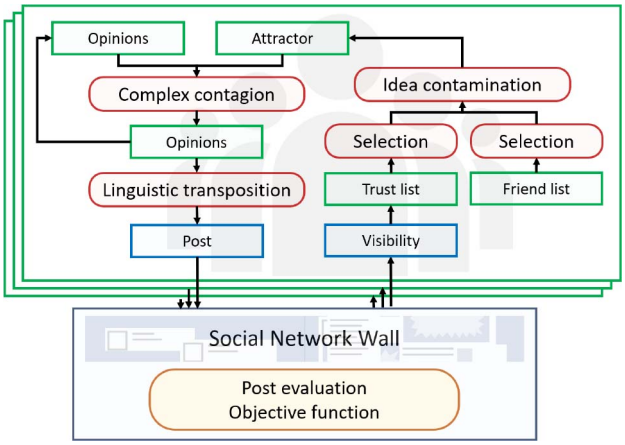

FIGURE 1. Social Network Optimization logic.

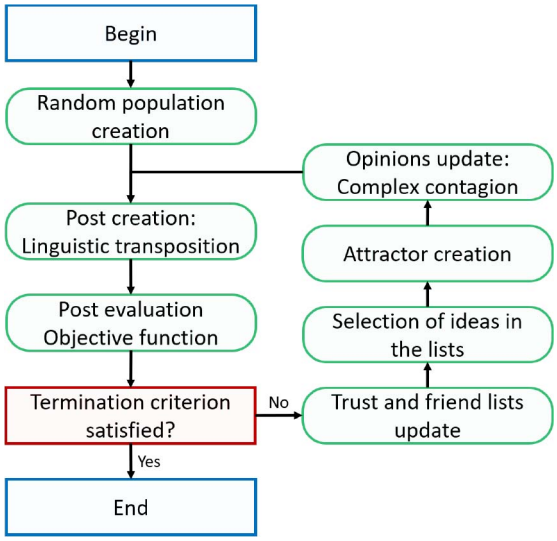

FIGURE 2. Social Network Optimization flow chart.

post from an opinion is called *linguistic transposition* and it is implemented by a gaussian mutation of the opinion.

At its turn, each post is evaluated by the social network and it receives a visibility value (the cost value of the problem) that indicates how much it is probable that another user can read it [39].

The online interaction takes place through two different networks: the *friend* one, characterized by strong connections among users and by a slow evolution rate, and the *trust network*, characterized by weaker interactions and by an evolution based on the posts' visibility value. Both these networks are updated dynamically during the iterations.

Each user exchanges opinions with other individuals, being in the same time influenced by both the networks. The interaction is based on a selection and combination process that creates the attractor, i.e., a mix of the ideas deriving from the two users' networks.

The final operator is the complex contagion, that emulates the influencing process in real social networks:

$$\mathbf{o}(t+1) = \mathbf{o}(t) + \alpha[\mathbf{o}(t) - \mathbf{o}(t-1)] + \beta[\mathbf{a}(t) - \mathbf{o}(t)] \quad (1)$$

where $\mathbf{o}$ is the user opinion and $\mathbf{a}$ is the attractor. Both of them are N-dimensional vectors, where N is the number of optimization variables.

Figure 2 shows the flow chart of SNO that summarizes the process described above.

Before applying the SNO to the reflectarray antenna problem, two preliminary analyses have been carried on: a parametric test on the complex contagion operator and its dependence on the parameters α and β, and a comparison with other EAs on standard benchmark functions.

A. PARAMETRIC ANALYSIS ON COMPLEX CONTAGION OPERATOR

As for other EAs, also the SNO performance is highly affected by the selection of the working parameters; from eq. 1, it appears that the parameters α and β determine how much the evolution of the opinion associated to each member of the network depends on the opinion itself at previous steps and by the attractor. Their effect has been analyzed applying the SNO to four different benchmark functions, the Ackley, Rastrigin, Schwefel-226, and Sinc functions [1], all with dimension $N_D = 20$; the parameter α has been varied over the interval $[-1, 1]$, while β between 0 and 2. Both α and β are sampled with 100 points in their domain and for each set of parameters, 50 independent trials have been run, each with a maximum number of 5000 objective function calls.

Figure 3 shows the results of the parametric analysis, through a color map representation of the average value over the 50 trials of the cost function, evaluated for each set of parameters. The optimal values of α, β depend on the objective function, and it is indicated in the plots by the black circle: the choice of one of these optimal couples of values for α, β guarantees a good convergence of the algorithm on a specific benchmark function or at most for the class of objective functions it represents. Vice versa, the smaller black dot is located in correspondence of the set of parameters that gives the best trade-off results among the four analyzed functions; note that the two couples of values for $[\alpha, \beta]$ represented in each plot of Fig. 3 are not so far each other, except for the Ackley function.

It is interesting to observe that the choice $\alpha = 0$ provides a good performance, even if not the best possible one but for Rastrigin and Schwefel-226 functions. This is an interesting point, because it changes the behavior of the algorithm: in fact, the α parameter can be associated to the inertia factor of PSO. When $\alpha \to 0$ the algorithm becomes closer to GA, since the complex contagion operator, with $\alpha = 0$ becomes:

$$\mathbf{o}(t+1) = \mathbf{o}(t) + \beta[\mathbf{a}(t) - \mathbf{o}(t)] \quad (2)$$

i.e.:

$$\mathbf{o}(t+1) = (1-\beta)\mathbf{o}(t) + \beta\mathbf{a}(t) \quad (3)$$

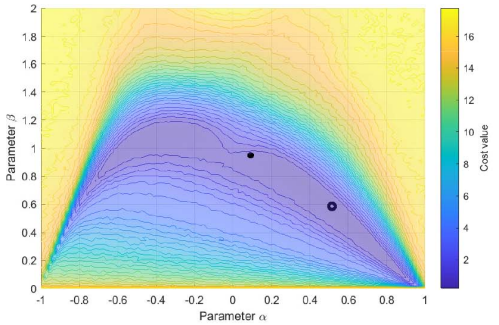

(a) Ackley function.

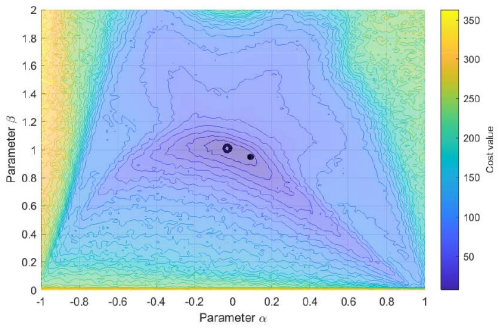

(b) Rastrigin function.

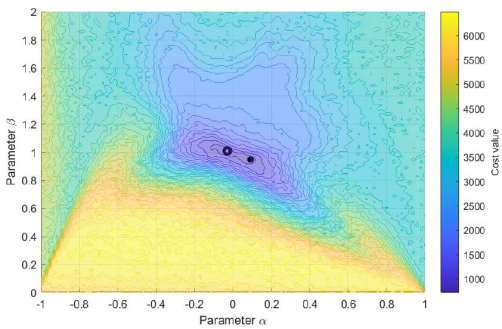

(c) Schwefel-226 function

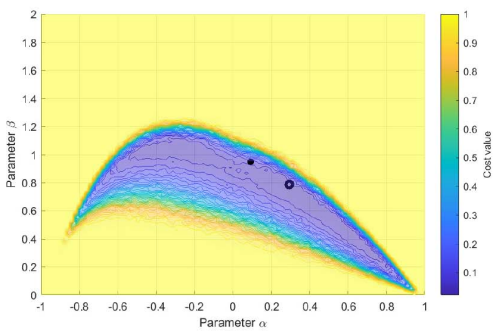

(d) Sinc function

FIGURE 3. Parametric analysis of the α and β parameters of SNO. The black circle is the optimal parameter set for each function, while the smaller black dot is the set of parameters that guarantees the better trade-off on the four here analyzed functions.

It means that, in this condition, the opinion at the new iteration is a weighted sum between the previous step opinion and attracting idea, while the user past history has no influence.

TABLE 1. Comparison between the SNO and other four optimization algorithms applied to benchmark functions.

		Ackley	Rastrigin	Schwefel-226	SincN
GA	mean	2.4	71.6	2809	0.732
	std	0.21	14.4	506	0.317
	test	-	-	-	-
PSO	mean	11.2	146	3340	1
	std	2	44	602	0
	test	-	-	-	-
mBBO	mean	2.84	15.3	257	0.453
	std	0.36	3	88	0.265
	test	-	-	+	-
SGA	mean	0.979	11.4	1057	0.73
	std	0.599	4	247	0.401
	test	-	+	-	-
SNO	mean	0.568	13.7	906	0.0709
	std	0.174	3.8	223	0.0412

B. COMPARISON ON STANDARD BENCHMARKS

After having identified the optimal set of parameters, the SNO performance has been assessed through the comparison with others well-established algorithms, such as the GA and the PSO [40]. Moreover, other two approaches, less popular, but with good performance have also been considered: the M_QC_{10}-BBO, a modified version of the Biogeography Based Optimization (BBO) [41] with improved exploration feature thanks to the introduction of the cataclysm operator [42], and the Stud-Genetic Algorithm (SGA) [43] that has shown better exploitation and local exploration capabilities with respect to other GAs.

The comparison has been done on the same benchmarks used for the parametric analysis. Also in these cases, 5000 objective function calls have been set as the termination criterion, while 50 independent trials have been performed for each algorithm, to obtain statistical reliability.

In Table 1, the mean value and the standard deviation evaluated for the five different algorithms are reported. The last line of each algorithm is the comparison with SNO, which is performed by means of a Wilcoxon signed rank test [44]. A "+" sign means that according to the test the considered algorithm outperforms SNO, a "=" means that both the algorithms show comparable performance, while a "−" means that SNO outperforms the considered algorithm.

The performance of SNO is remarkably better for functions that require high exploitation (Ackley and Sinc in particular), while for Rastrigin and for Schwefel-226 it is not worse than that of SGA and M_QC_{10}-BBO. This implies that SNO is a very robust algorithm since it performs well on different types of objective functions. Moreover, its standard deviation is very low for almost all the functions: this is very important because it proves the algorithm reliability, a crucial aspect in antenna optimization in which the computational time is very high.

III. OPTIMIZATION PROBLEM

The considered optimization problem consists in designing a RA with scanning capabilities over a predefined angular

range $[\theta^s_{min}, \theta^s_{max}]$ in the elevation plane. This means to find the optimal distribution for the RA patches, that guarantees a reduced degradation of the antenna radiating performance over $[\theta^s_{min}, \theta^s_{max}]$.

Beam-scanning capabilities in reflectarrays can be achieved employing active elements in their unit-cells, such as varactor diodes [45], [46], pin diodes [47], liquid crystals [48] or MEMS switches [49]. Despite their improved beam control performance, active RAs present some significant drawbacks: the lower efficiency due to the high losses, the design complexity and the fabrication cost. Alternatively, a less complex solution can be obtained by using passive RAs with mechanical beam-steering mechanisms [26], [50]–[54]. The beam-scanning can be implemented mechanically controlling the height of the slotted patch [52], by simply adjusting the rotations of the unit-cells [53], or more commonly by rotating the feed along a circular arc [26], [51], with eventually the addition of a rotation of the RA, to increase the scanning range [54]. In all these cases the interval $[\theta^s_{min}, \theta^s_{max}]$ is assumed symmetrical with respect to the broadside ($\theta^s_{min} = -\theta^s_{max}$), with the advantage that the starting position of the feed is center-fed, even if this choice is responsible for a degradation of the radiation pattern for pointing direction close to the broadside one, due to the blockage of the feed. A well-established technique to obtain the beam steering moving the feed is that of designing a bifocal RA [26], [50], where the patch distribution tries to compensate the phase of the field impinging from two different directions, generally $-\theta^s_{max}$ and θ^s_{max}. As a result, the antenna performance decreases with the moving from the pointing directions used in the design, and the maximum gain suffers for a reduction over the entire angular range. As an alternative, the use of a multi-objective PSO [26] has been proposed, and it provides good solutions, but at the cost of a high computational effort. This has been reduced with the approach proposed in [51], where the multibeam phase matching method (PMM) is used to evaluate the desired aperture phase distributions and the PSO is adopted only to optimize the feed offset angles and the reference phases. The results relative to a very small square RA ($8\lambda_0 \times 8\lambda_0$) prove that the proposed method outperforms the bifocal design.

Here, the possibility to have a scanning coverage from $-\theta^s_{max}$ to θ^s_{max} is taken into account simply observing that it corresponds to have a symmetrical distribution of the RA unit-cells; it is therefore possible to optimize the RA performance over a positive scanning sub-range and use the symmetries to cover also the negative one. This solution has two advantages: 1) to reduce the pointing directions in correspondence of which the RA radiation pattern must be optimized and 2) to reduce the optimization problem dimension. The here analyzed RA consists of 24×24 squared patches located in a grid whose cell size is equal to $\lambda/2$, at 30 GHz. The patches are printed on a Diclad© 527 substrate with $\epsilon_r = 2.55$ and a thickness of 0.8 mm. The unit-cell has been assumed to be embedded in a periodic lattice, and the magnitude and phase of the reflection coefficient Γ have been computed with CST Microwave Studio© as a function of the side W of the patch. When illuminated by an orthogonal incident wave, the cell can provide almost everywhere 0 dB of magnitude and a total variation of 300° for the phase of Γ over the entire interval of variation for W [36].

The reflective surface is illuminated by a smooth-wall horn [55] designed to work in a frequency range centered at $f_0 = 30$ GHz, whose radiation pattern in the two principal planes that can be modeled by $cos(\theta)^q$ function, with $q = 12.5$. The focal distance f/D is 1.2, to have a proper illumination of the RA surface.

The starting position of the feed is almost specular to the direction of maximum radiation of the RA identified by the lowest extreme of the scanning range, assumed to be $\theta^s_{min} = 10°$. Then, the feed moves along a circular arc, to cover the entire scanning range, up to $\theta^s_{max} = 40°$. To guarantee that the designed RA maintains almost the same performance for all the pointing directions in the range, the RA radiation patterns for four different values of the angle of maximum radiation inside $[\theta^s_{min}, \theta^s_{max}]$, i.e., $\theta_{max} = 10°, 20°, 30°, 40°$ have been considered in the optimization process.

The considered design variables are of two types:

- the size of the patches, thanks to which it is possible to control the phase of the reflected field; due to the symmetries of the system, the number of independent patch size is reduced from 576 to 144.
- the Beam Deviation Factor (BDF), which is defined as the ratio between the direction of maximum radiation θ_{max} and the incident angle θ_{inc}. Ideally, $BDF = 1$. The number of beam deviation factors depends on the number of considered directions of maximum radiation, in this case it is equal to four. While in [51] a single BDF is just used to minimize the RA phase errors, here they represent four more degrees of freedom, that the SNO can use to optimize the RA radiation patterns.

IV. DESIGN OF THE OPTIMIZATION ENVIRONMENT

In this Section, the design of the optimization environment is described. Its general framework is firstly introduced, then several parts are deeply analyzed: in particular, the definition of the cost function, the effect of the population size and the type of box boundary constraints are investigated.

A. OPTIMIZATION ENVIRONMENT

The optimization environment is composed by a set of interacting parts, that affects the overall performance of the optimization process: their proper design is fundamental for reducing the computational time required for obtaining a high quality final solution.

The optimization environment is composed by two main blocks. The first is the optimization algorithm, that is characterized by its operators, the number and type of optimization variables, and in which it is important to set the number of function calls. The second block is the objective function, that is, in turns, composed by several other parts, i.e., the

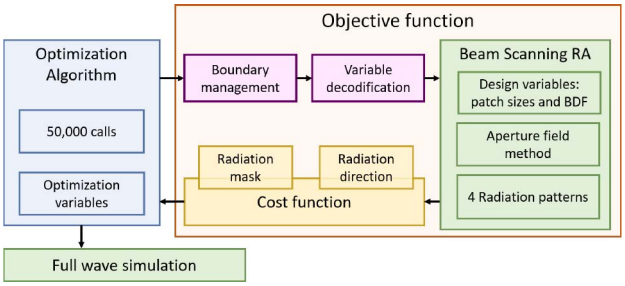

FIGURE 4. Optimization scheme for the design of a beam-scanning reflectarray.

constraint management method, the variable decodification, the optimization problem, and the cost function.

A block diagram of the optimization environment for the beam-scanning problem is shown in Figure 4.

In the problem addressed here, the first aspect that should be considered in the definition of the optimization environment is related to the required computational time for computing the antenna performance. In fact, it is almost impossible to use the full-wave simulation inside the optimization loop, since it would increase dramatically the computational cost of the whole procedure making it unfeasible. For this reason, the aperture field method has been used during the optimization process, and a full-wave approach is only adopted for validating the designed RA configuration performance.

The second aspect is related to the different nature of the design variables. They have different domains of definition, and therefore in the optimization algorithm variables normalized in the range [0, 1] are used. This choice also simplifies the definition of the box constraint conditions, thus the decoding of the variables is done after their application [56].

The third and last element that influences the definition of the optimization environment is the cost function used to describe the considered problem. Strictly speaking, the design of a beam-scanning RA is a multi-objective problem since the aims of the procedure are:

- to optimize four different radiation patterns, one for each considered direction of maximum radiation;
- to minimize the difference between the actual direction of maximum radiation and the desired one.

B. PERFORMANCE PARAMETERS AND COST DEFINITION

In Section III it has already been pointed out that to guarantee a good radiating performance over the entire interval $[\theta^s_{min}, \theta^s_{max}]$, the radiation patterns for four different pointing directions are considered in the optimization process. For each of them, it is possible to define two performance parameters that depend on the design variables $\mathbf{d}$ (patches size plus BDFs) and can be used to evaluate the goodness of a given solution. The first one is the integral of the radiation pattern exceeding a predefined mask:

$$c_1(\mathbf{d}) = \iint \Delta(\theta, \phi) d\theta d\phi \tag{4}$$

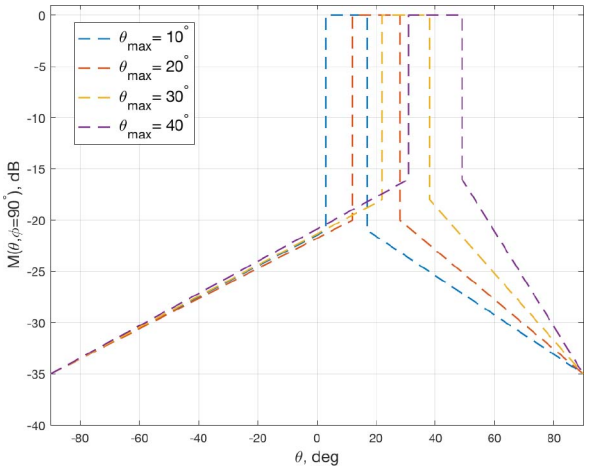

FIGURE 5. E-plane view of the masks (one for each of the considered pointing direction) adopted in the optimization process.

where Δ is the error, defined in terms of the Heavyside function H:

$$\Delta(\theta, \phi) = [E(\theta, \phi) - M(\theta, \phi)]H(E(\theta, \phi) - M(\theta, \phi)) \tag{5}$$

Since four different directions of maximum radiation are considered, four different masks are used. Their cross-sectional view in the vertical plane, where the beam scanning occurs, is shown in Fig. 5. To better control the Side Lobe Level (SLL), the mask out of the main beam decrease linearly. Moreover, they are not exactly equal: the effects of the beam steering, responsible for the widening of the main beam and for the increasing of side lobes, are taken into account, to guide the optimization algorithm to a feasible solution and to improve its convergence.

Moreover, differently to what has been done in the related literature (see, e.g., [14] and the references therein), a second quantity is also considered, i.e., the scan angle error, expressed as the squared value of the difference between the desired direction of maximum radiation θ_s and the actual one, θ_{max}:

$$c_2(\mathbf{d}) = \Delta\theta_s = \left[(\theta_s - \theta_{max})\frac{180}{\pi}\right]^2 \tag{6}$$

These two objective functions can be used to properly guide the optimization process [36]. In fact, the integral error between the mask and the radiation pattern is a very common cost value, but it cannot detect accurately the scan angle error. For this reason, the second objective function has been added to increase the effectiveness of the procedure.

The total number of costs is therefore equal to eight and the problem is a real multi-objective one. In opposite to what proposed in [26], where only two objectives are considered and a Multi-Objective PSO is used for the antenna optimization, here they are combined together with a two-level scalarization procedure; for each of the four considered scan angles, the two costs (4) and (6) are first associated:

$$c_{s,i}(\mathbf{d}) = c_1(\mathbf{d}) + \lambda c_2(\mathbf{d}) \tag{7}$$

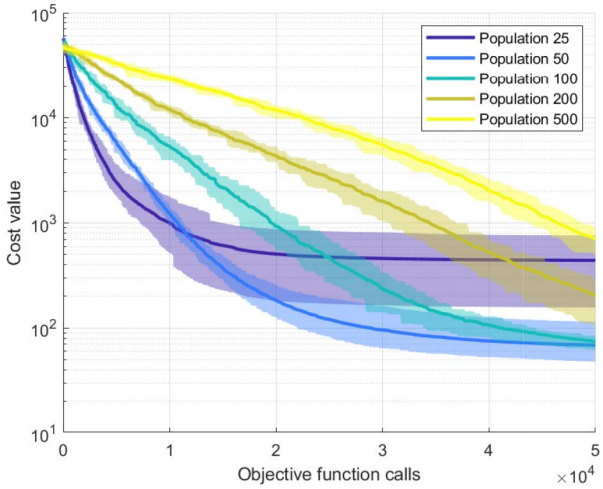

FIGURE 6. Convergence curves with different population size of SNO. The thick line is the average value, and the bands represent the 80% confidence level on the independent trials.

where λ is a weight that allows to control the relative importance of the two objectives.

Then, the four equations of type (7), are merged in a single cost function, that is returned to the optimizer. It is defined as

$$C = \lambda_1 c_{10} + \lambda_2 c_{20} + \lambda_3 c_{30} + \lambda_4 c_{40} \tag{8}$$

where λ_i are four weights that could be chosen in such a way to improve the effectiveness of the optimization process. In fact, the type of coordinates used in the radiation pattern evaluation makes the optimizer more sensible to errors concentrated in the central region of the radiation pattern, and this results in a faster optimization of the radiation patterns with closer to broadside direction of maximum radiation.

C. DEFINITION OF POPULATION SIZE

The population size is a very important parameter that should be used to improve the performance of SNO since it is one of the most effective drivers of the trade-off between exploration of the search space and exploitation of the available information.

Here, five different population sizes have been tested, consisting in 25, 50, 100, 200 and 500 individuals, respectively. In all the tests, 16 independent trials have been performed, each with a $N_c = 50{,}000$ objective function calls. Since N_c is given by the product between the population size N_p and the number of iteration N_i, to keep it constant at the increasing of N_p, N_i has to decrease. While the convergence of an evolutionary algorithm is commonly evaluated for a fixed value of N_i, the criterion adopted here guarantees that the computational cost for each trial varies of no more than the 0.95% even when the population size changes.

Figure 6 shows the convergence of the different tests. The thick line is the average result, while the colored area is limited by the 10% and the 90% percentile of the trials.

From these results, it is clear that the performance of the algorithm is highly affected by the population size: larger populations slow down the convergence, while low sizes guarantee a faster convergence at the beginning of the optimization, but this speed slows down very quickly and leads to a great dispersion of the final results.

The two most interesting population sizes are 50 and 100. When $N_p = 50$ the best final result is achieved, but the standard deviation is quite high, thus the average value is comparable with the results with 100 individuals. This last case is very interesting because the standard deviation is very low during the entire optimization process. It is worth to notice that the reduced standard deviation is a very important aspect for the optimization system scalability: in fact, when the computational time grows, it is possible to reduce the number of independent trials to be performed.

D. ANALYSIS OF BOX CONSTRAINTS

The problem is characterized by box constraints that limit the upper and the lower allowed values for each design variable. The different methods that can be used for managing this kind of constraints affect the convergence performance of the whole algorithm. In particular, in the antenna problem their influence is amplified by the fact that the phase of the reflection coefficient, depending on one of the two types of considered variables, i.e., the size of the patches in the unit cells, has a periodic behavior.

Here, four different box boundary functions have been tested: the impenetrable wall, the rebounding wall, the eliminating wall and the closed search space.

The penalty approach cannot be used in this specific application because the physical proprieties of the patches are not computed outside the feasible search domain.

The first box constraint approach is the impenetrable wall, that curtails the component exceeding the search space to its limits:

$$\tilde{x}_i = \begin{cases} L_i, & x_i < L_i \\ U_i, & x_i > U_i \\ x_i, & \text{otherwise} \end{cases} \tag{9}$$

where $\tilde{x}_i$ is the i-th component of the modified candidate solution, x_i is the candidate solution, U_i is the upper bound for the i-th component and L_i is the lower bound.

Another approach is to model the boundary as an elastic bound: the components exceeding the bounds, are reflected inside the domain:

$$\tilde{x}_i = \begin{cases} L_i + |L_i - x_i|, & x_i < L_i \\ U_i - |U_i - x_i|, & x_i > U_i \\ x_i, & \text{otherwise} \end{cases} \tag{10}$$

In this condition, the exploration is slightly increased; however, the capability of finding the best on the search space limits is drastically reduced.

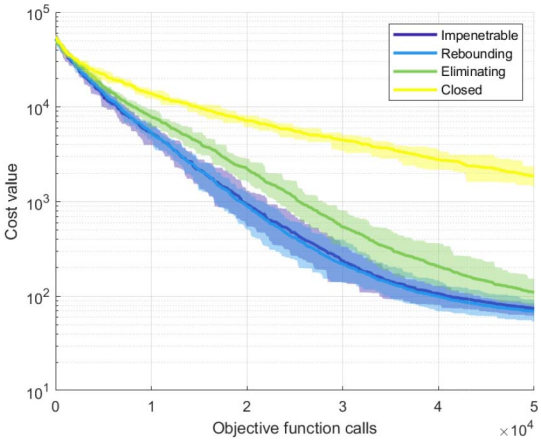

FIGURE 7. Comparison among the different convergence curves obtained with the four box boundary conditions.

Another possibility is to eliminate the components that exceed the search domain and to recreate them randomly:

$$\tilde{x}_i = \begin{cases} r, & x_i < L_i \\ r, & x_i > U_i \\ x_i, & \text{otherwise} \end{cases} \tag{11}$$

where r is a random value inside the search domain.

Finally, it is possible to define the search domain as it is a closed surface, and the boundary can be written in the following way:

$$\tilde{x}_i = \begin{cases} U_i - (L_i - x_i), & x_i < L_i \\ L_i + (x_i - U_i), & x_i > U_i \\ x_i, & \text{otherwise} \end{cases} \tag{12}$$

This condition is rarely used, but it can improve the optimization if the design variables refer to periodic elements (e.g., angles) or when local minima are close to the boundaries and, thus, this condition improves the exploration.

These four conditions have been applied to the antenna problem; 16 independent trials have been performed for each test and $N_c = 50{,}000$ is again used as termination criterion.

The results are shown in Figure 7, where the average convergence and the 80% confidence level are plotted for the four types of box constrains.

It is possible to notice that the closed wall has a much worst convergence starting from the first iterations. The eliminating wall is less effective with respect to the others because makes very difficult the exploitation of solutions with patch size close to the limit values. The other two conditions are characterized by a very similar convergence, and their difference can be better investigated analyzing the numerical results reported in Table 2, where the mean and the best values of the cost function as well as the standard deviation obtained with the four types of boundaries are reported.

The difference between the average value and the best results is very small, while the impenetrable wall has a much lower standard deviation. Due to the high computational cost of this problem, the stability of the algorithm has been preferred over a tiny improvement of the final solution.

TABLE 2. Comparison of the results obtained with the considered four types of box constrains.

Box condition	Mean	Standard deviation	Best result
Impenetrable	74.40	**7.893**	61.85
Rebounding	**69.71**	19.36	**51.29**
Eliminating	110.4	39.38	77.63
Closed	1867	396.8	1309

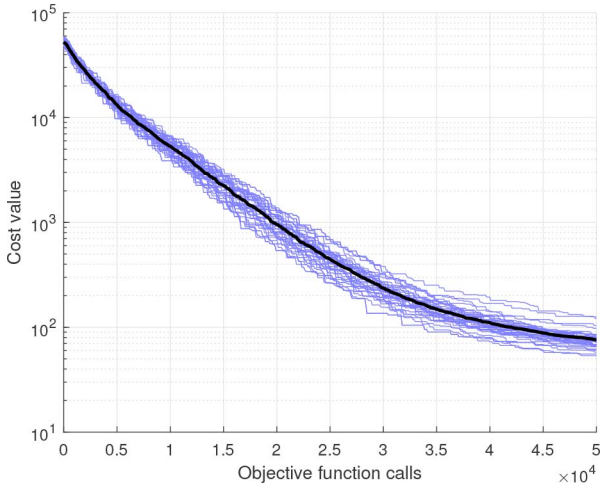

FIGURE 8. Convergence curves of 40 independent trials of SNO: the thin lines are the single trials, while the black line is the average convergence.

V. RESULTS AND DISCUSSION

Once that the optimization environment has been properly set, it has been applied to the design of a RA with feature as those described in Section III. The optimization with the SNO has been performed adding 24 independent trials to the 16 performed in the comparisons for further assess the algorithm stability. The convergence curves are shown in Figure 8. The thin lines are the independent trials, while the thick black line represents the average convergence. The adopted termination criterion is again $N_c = 50{,}000$. The optimization process has been performed using a PC with Intel Core i7-7820x @3.60GHz and exploiting MATLAB Parallel Computing Toolbox on 8 parallel cores [57].

The optimized solution is shown in Figure 9, where the entire antenna (RA + feed) is sketched, while the optimal values for the BDF, corresponding to the four considered directions of maximum radiation, are [0.89, 0.94, 0.95, 0.96].

The performance of SNO and of the optimized antenna configuration has been tested against those of other EAs, applied to the same problem, and performing the full-wave analysis of the antenna shown in Fig. 9. The obtained results are summarized in the following.

A. COMPARISON WITH OTHER EVOLUTIONARY ALGORITHMS

The SNO results have been first assessed against those obtained with the four EAs already considered in

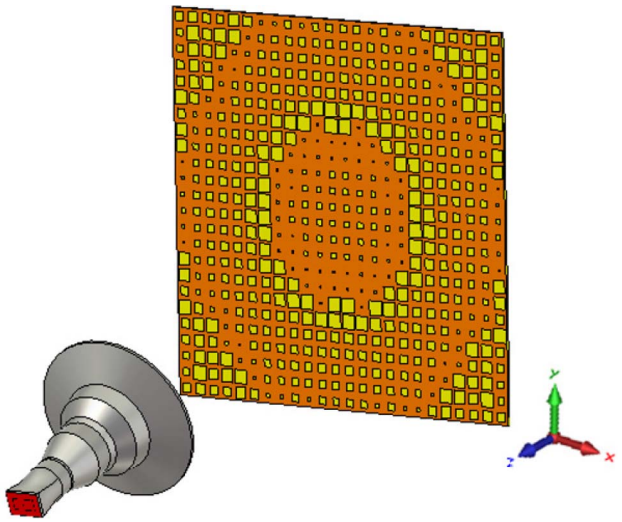

FIGURE 9. Layout of the 24 × 24 optimized RA.

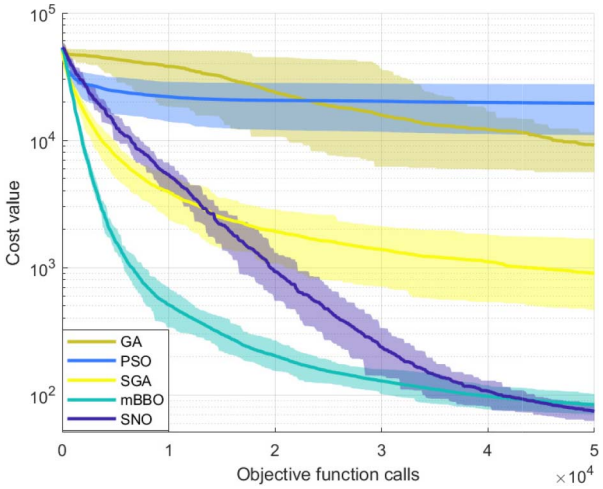

FIGURE 10. Comparison among the convergence of the five analyzed algorithms: for each of them the thick line represents the average value, while the coloured area is the 80% confidence level.

Section II-B. To perform a fair comparison, the value of user-defined parameters of all the algorithms have been preliminary identified by means of a parametric analysis on the same standard benchmarks used for SNO.

The used population size is 100 individuals for each algorithm and the termination criterion has been set to 50,000 objective function calls. This guarantees that the computational time required is almost the same for all the algorithms because the algorithm self-time (ranging from 1.2 second for the PSO to 3.3 seconds for the SNO) is negligible with respect to the total optimization time (ranging from 36750 seconds to 37250 seconds). All the optimization time are detailed in Table 3. For all the compared algorithms 16 independent trials have been performed, thus for SNO the trials used in Section IV have been here considered.

The convergence curves relative to the different algorithms are shown in Figure 10. The thick lines represent the average of the 16 trials, while the colored areas are delimited by the 10% and the 90% percentiles.

Traditional algorithms, such as PSO and GA perform poorly on this problem due to the large search space and the problem non-linearities. PSO has a very fast initial convergence, and then it stalls quickly in local minima. GA is characterized by a generally slower, but more constant speed.

The SGA performance is much better, even if the convergence rate drops very rapidly and, thus, the quality of the achieved final solution is relatively poorer than others.

The M_QC_{10}-BBO and the SNO perform much better than the other algorithms. The first one has a very fast initial convergence (up to one fifth of the optimization time), while SNO is more constant during almost all the optimization process has already pointed out by the curves in Fig. 8.

Table 3 shows a comprehensive comparison between the algorithms. For each of them, the mean final value, the standard deviation, the best cost and the average optimization time achieved over the 16 independent trials are reported. In addition, the comparison between the SNO and the other algorithms is carried out using two non-parametric statistical tests: the Wilcoxon signed rank test and the Friedman's test.

The results of the Wilcoxon test show that SNO outperforms all the other algorithms (indicated in the table with the sign "−"), while the Friedman's test p-values confirm the results [44].

Comparing the results for the M_QC_{10}-BBO and the SNO, it is possible to see that this last has better performance both in terms of average value and best solution. Moreover, its standard deviation is lower, and this further confirms its good stability also in this computationally intensive application.

B. SOLUTION ASSESSMENT

Even if the results summarized in Section V-A prove the effectiveness of the SNO, which outperforms the other considered EAs, the correctness of the designed configuration has also to be checked. Therefore, the RA in Fig. 9 has been simulated with CST Microwave Studio©, and the obtained radiation patterns have been compared with the masks and the patterns directly evaluated through the optimization process.

In Figure 11 the results in the E-plane are shown, while in Figure 12 those in the H-plane. The radiation patterns evaluated with the full-wave approach satisfy the masks almost everywhere and are in good agreement with those obtained at the end of the optimization, proving the effectiveness of the SNO and of the optimization environment discussed in Section IV. The side lobes exceeding the mask in the H-plane, for the case $\theta_{max} = 10°$, are due to the blockage of the feed, that has not been taken into account in the optimization. It is worth to notice that thanks to the introduction of the cost function 6, the finding pointing directions θ_{max} are from the desired ones θ_s no more than 0.5° far and that in the case of the radiation pattern for $\theta_{max} = 40°$ in

TABLE 3. Comparison between SNO and other optimization algorithms.

Algorithm	Mean	Standard deviation	Best result	Optimization time [s]	Wilcoxon test	Friedman's test
GA	9131.54	6338.5082	3430.362	36770	-	6.3342e-05
PSO	19507.616	6369.737	5122.6799	36750	-	6.3342e-05
SGA	901.5417	442.449	247.3504	37020	-	6.3342e-05
mBBO	84.0504	11.2737	65.1102	37170	-	0.13361
SNO	74.4034	7.8928	61.8466	37250		

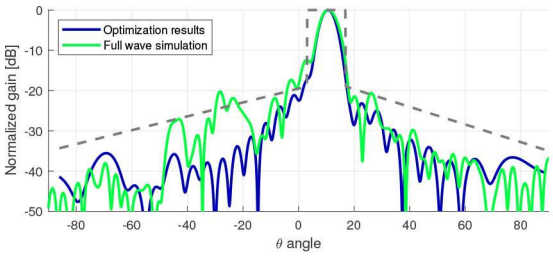

(a) $\theta_{max} = 10°$

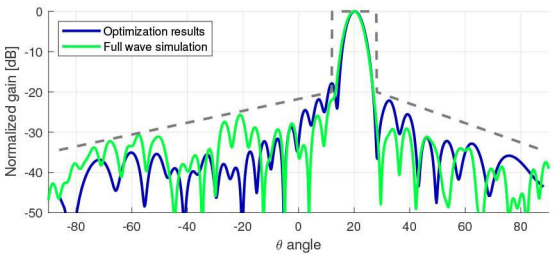

(b) $\theta_{max} = 20°$

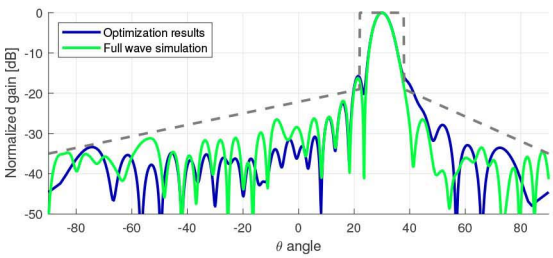

(c) $\theta_{max} = 30°$

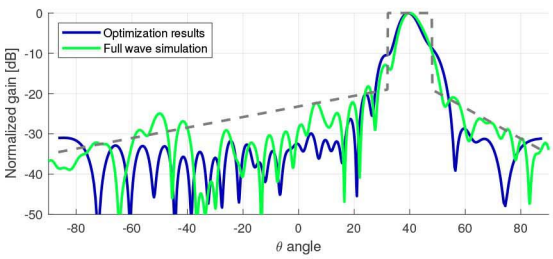

(d) $\theta_{max} = 40°$

FIGURE 11. Radiation patterns in *E*-plane: comparison among those evaluated during the optimization process, the full-wave simulation and the masks used for the optimization.

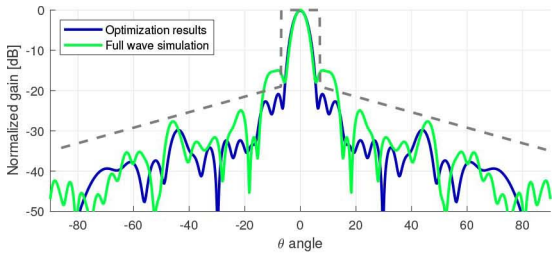

(a) $\theta_{max} = 10°$

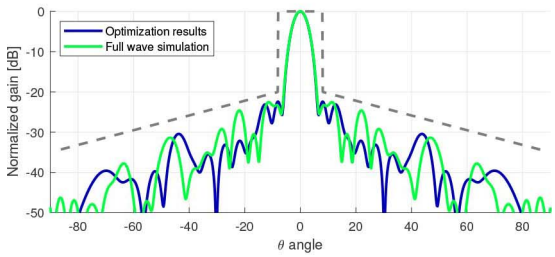

(b) $\theta_{max} = 20°$

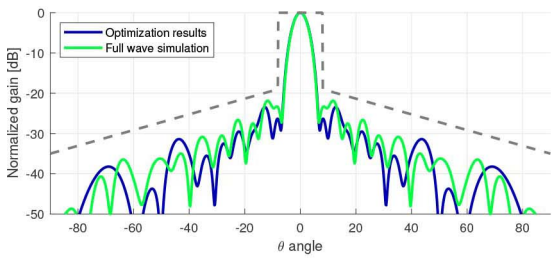

(c) $\theta_{max} = 30°$

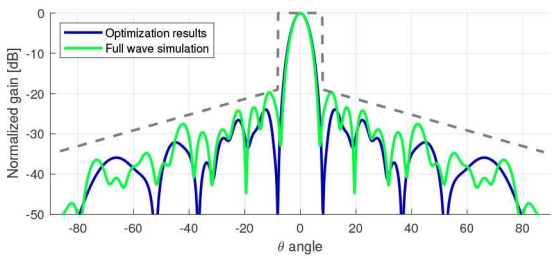

(d) $\theta_{max} = 40°$

FIGURE 12. Radiation patterns in *H*-plane: comparison among those evaluated during the optimization process, the full-wave simulation and the masks used for the optimization.

the E-plane, the main lobe obtained with the full-wave simulation of the RA is even narrower than the one computed by the optimization process.

In Table 4 the maximum gain for different pointing directions and its variation over the considering scanning range are reported. These values, evaluated with the full-wave simulation of the RA, show that the gain is maximum for $\theta_{max} = 20°$, and this confirms the effect of the feed blockage for smaller pointing angles, and that the total variation of the gain over the considered $[\theta^s_{min}, \theta^s_{max}]$ interval is very small, since it is equal to 1.6 dB.

TABLE 4. Maximum gain for different pointing directions.

θ_{max} = 10°	θ_{max} = 20°	θ_{max} = 30°	θ_{max} = 40°	ΔG
28.7 dBi	29.2 dBi	29.1 dBi	27.6 dBi	1.6 dB

Finally, the performances of the reflectarray designed with SNO are compared with those of the configuration in [51]. The RA in [51] has a square shape, as the one considered here, but a smaller size ($8\lambda_0 \times 8\lambda_0$) with respect to the solution presented here; since at the increasing of the reflectarray size (here 3/2 times larger than the solution in [51]) the phase distribution on the RA surface is more sensitive to the variation of the direction of arrival of the incident field, a degradation of the whole antenna performance can be expected. Nevertheless, the antenna in [51] is characterized by a fluctuation of the maximum gain over a range of variation for the pointing direction with the same amplitude of the one considered here equal to 1.95 dB, while the side lobes are comparable with those of the optimized antenna for $\theta_{max} = 10°$ and the maximum scanning angle, while are higher for the directions of pointing between these two extremes.

VI. CONCLUSION

In this article, the Social Network Optimization has been applied to the design of a beam-scanning passive reflectarray antenna.

The entire optimization environment has been analyzed, testing different algorithm population sizes and four different box boundary conditions; moreover, the performance of SNO has been compared with those of other EAs (GA, PSO, SGA and $M_Q C_{10}$-BBO).

In all these tests, the high robustness and accuracy of the SNO is proven. Then the obtained optimal solution has been assessed with its full-wave simulation. Also in this last test, the quality of the solution obtained with the SNO has been confirmed.

The designed optimization environment makes the system easily scalable to larger reflectors with more degrees of freedom, thus the first follow-up of this work is the optimization of a larger antenna to test how the system can be scaled.

Finally, a further follow-up is the assessment of the method through the manufacturing of a prototype and its experimental characterization.

REFERENCES

[1] D. Simon, *Evolutionary Optimization Algorithms*. Hoboken, NJ, USA: Wiley, 2013.

[2] S. K. Goudos, C. Kalialakis, and R. Mittra, "Evolutionary algorithms applied to antennas and propagation: A review of state of the art," *Int. J. Antennas Propag.*, vol. 2016, Aug. 2016, Art. no. 1010459.

[3] R. L. Haupt and D. H. Werner, *Genetic Algorithms in Electromagnetics*. Hoboken, NJ, USA: Wiley, 2007.

[4] F. J. Ares-Pena, J. A. Rodriguez-Gonzalez, E. Villanueva-Lopez, and S. Rengarajan, "Genetic algorithms in the design and optimization of antenna array patterns," *IEEE Trans. Antennas Propag.*, vol. 47, no. 3, pp. 506–510, Mar. 1999.

[5] P. Rocca, G. Oliveri, and A. Massa, "Differential evolution as applied to electromagnetics," *IEEE Antennas Propag. Mag.*, vol. 53, no. 1, pp. 38–49, Feb. 2011.

[6] J. Robinson and Y. Rahmat-Samii, "Particle swarm optimization in electromagnetics," *IEEE Trans. Antennas Propag.*, vol. 52, no. 2, pp. 397–407, Feb. 2004.

[7] W. T. Li, X. W. Shi, Y. Q. Hei, S. F. Liu, and J. Zhu, "A hybrid optimization algorithm and its application for conformal array pattern synthesis," *IEEE Trans. Antennas Propag.*, vol. 58, no. 10, pp. 3401–3406, Oct. 2010.

[8] X. Jia and G. Lu, "A hybrid taguchi binary particle swarm optimization for antenna designs," *IEEE Antennas Wireless Propag. Lett.*, vol. 18, pp. 1581–1585, 2019.

[9] M. E. Yigit and T. Giinel, "Pattern synthesis of linear antenna array via a new hybrid taguchi-genetic-particle swarm optimization algorithm," in *Proc. IEEE 18th Mediterr. Microw. Symp. (MMS)*, Istanbul, Turkey, 2018, pp. 17–21.

[10] M. F. Pantoja, P. Meincke, and A. R. Bretones, "A hybrid genetic-algorithm space-mapping tool for the optimization of antennas," *IEEE Trans. Antennas Propag.*, vol. 55, no. 3, pp. 777–781, Mar. 2007.

[11] J. Yang, P. Yang, F. Yang, Z. Xing, X. Ma, and S. Yang, "A hybrid approach for the synthesis of nonuniformly-spaced linear subarrays," *IEEE Trans. Antennas Propag.*, early access, Jul. 16, 2020, doi: 10.1109/TAP.2020.3008664.

[12] S.-R. Zhang, Y.-X. Zhang, and C.-Y. Cui, "Efficient multiobjective optimization of time modulated array using a hybrid particle swarm algorithm with convex programming," *IEEE Antennas Wireless Propag. Lett.*, early access, Aug. 11, 2020, doi: 10.1109/LAWP.2020.3014366.

[13] J. Huang and J. A. Encinar, *Reflectarray Antennas*. Hoboken, NJ, USA: Wiley, 2008.

[14] P. Nayeri, F. Yang, and A. Z. Elsherbeni, *Reflectarray Antennas: Theory, Designs and Applications*. Hoboken, NJ, USA: Wiley, 2018.

[15] D. M. Pozar, S. D. Targonski, and H. Syrigos, "Design of millimeter wave microstrip reflectarrays," *IEEE Trans. Antennas Propag.*, vol. 45, no. 2, pp. 287–296, Feb. 1997.

[16] O. M. Bucci, G. Franceschetti, G. Mazzarella, and G. Panariello, "Intersection approach to array pattern synthesis," *IEE Proc. H, Microw. Antennas Propag.*, vol. 137, no. 6. pp. 349–357, Dec. 1990.

[17] O. M. Bucci, G. D'Elia, G. Mazzarella, and G. Panariello, "Antenna pattern synthesis: A new general approach," *Proc. IEEE*, vol. 82, no. 3, pp. 358–371, Mar. 1994.

[18] R. Vescovo, "Reconfigurability and beam scanning with phase-only control for antenna arrays," *IEEE Trans. Antennas Propag.*, vol. 56, no. 6, pp. 1555–1565, Jun. 2008.

[19] J. A. Encinar and J. A. Zornoza, "Three-layer printed reflectarrays for contoured beam space applications," *IEEE Trans. Antennas Propag.*, vol. 52, no. 5, pp. 1138–1148, May 2004.

[20] E. Carrasco, M. Arrebola, J. A. Encinar, and M. Barba, "Demonstration of a shaped beam reflectarray using aperture-coupled delay lines for LMDS central station antenna," *IEEE Trans. Antennas Propag.*, vol. 56, no. 10, pp. 3103–3111, Oct. 2008.

[21] P. Nayeri, F. Yang, and A. Z. Elsherbeni, "Design and experiment of a single-feed quad-beam reflectarray antenna," *IEEE Trans. Antennas Propag.*, vol. 60, no. 2, pp. 1166–1171, Feb. 2012.

[22] H. Yang *et al.*, "A 1-bit 10 × 10 reconfigurable reflectarray antenna: Design, optimization, and experiment," *IEEE Trans. Antennas Propag.*, vol. 64, no. 6, pp. 2246–2254, Jun. 2016.

[23] Y. Aoki, H. Deguchi, and M. Tsuji, "Reflectarray with arbitrarily-shaped conductive elements optimized by genetic algorithm," in *Proc. IEEE Int. Symp. Antennas Propag. (APSURSI)*, Spokane, WA, USA, 2011, pp. 960–963.

[24] D. Kurup, M. Himdi, and A. Rydberg, "Design of an unequally spaced reflectarray," *IEEE Antennas Wireless Propag. Lett.*, vol. 2, pp. 33–35, 2003.

[25] P. Nayeri, F. Yang, and A. Z. Elsherbeni, "Design of single-feed reflectarray antennas with asymmetric multiple beams using the Particle Swarm Optimization method," *IEEE Trans. Antennas Propag.*, vol. 61, no. 9, pp. 4598–4605, Sep. 2013.

[26] P. Nayeri, F. Yang, and A. Z. Elsherbeni, "Bifocal design and aperture phase optimizations of reflectarray antennas for wide-angle beam scanning performance," *IEEE Trans. Antennas Propag.*, vol. 61, no. 9, pp. 4588–4597, Sep. 2013.

[27] Y. Mao, S. Xu, F. Yang, and A. Z. Elsherbeni, "A novel phase synthesis approach for wideband reflectarray design," *IEEE Trans. Antennas Propag.*, vol. 63, no. 9, pp. 4189–4193, Sep. 2015.

[28] M. Zhou, S. B. Sørensen, O. S. Kim, E. Jørgensen, P. Meincke, and O. Breinbjerg, "Direct optimization of printed reflectarrays for contoured beam satellite antenna applications," *IEEE Trans. Antennas Propag.*, vol. 61, no. 4, pp. 1995–2004, Apr. 2013.

[29] M. Zhou, O. Borries, and E. Jørgensen, "Design and optimization of a single-layer planar transmit-receive contoured beam reflectarray with enhanced performance," *IEEE Trans. Antennas Propag.*, vol. 63, no. 4, pp. 1247–1254, Apr. 2014.

[30] M. Zhou *et al.*, "The generalized direct optimization technique for printed reflectarrays," *IEEE Trans. Antennas Propag.*, vol. 62, no. 4, pp. 1690–1700, Apr. 2014.

[31] D. R. Prado *et al.*, "Efficient crosspolar optimization of shaped-beam dual-polarized reflectarrays using full- wave analysis for the antenna element characterization," *IEEE Trans. Antennas Propag.*, vol. 65, no. 2, pp. 623–635, Feb. 2017.

[32] D. R. Prado, J. A. López-Fernández, G. Barquero, M. Arrebola, and F. Las-Heras, "Fast and accurate modeling of dual-polarized reflectarray unit cells using support vector machines," *IEEE Trans. Antennas Propag.*, vol. 66, no. 3, pp. 1258–1270, Mar. 2018.

[33] D. R. Prado, J. A. López-Fernández, M. Arrebola, and G. Goussetis, "Support vector regression to accelerate design and crosspolar optimization of shaped-beam reflectarray antennas for space applications," *IEEE Trans. Antennas Propag.*, vol. 67, no. 3, pp. 1659–1668, Mar. 2019.

[34] D. R. Prado, J. A. López-Fernández, M. Arrebola, M. R. Pino, and G. Goussetis, "Wideband shaped-beam reflectarray design using support vector regression analysis," *IEEE Antennas Wireless Propag. Lett.*, vol. 18, pp. 2287–2291, 2019.

[35] G. Oliveri, A. Gelmini, A. Polo, N. Anselmi, and A. Massa, "System-by-design multiscale synthesis of task-oriented reflectarrays," *IEEE Trans. Antennas Propag.*, vol. 68, no. 4, pp. 2867–2882, Apr. 2020.

[36] A. Niccolai, R. Zich, M. Beccaria, and P. Pirinoli, "SNO based optimization for shaped beam reflectarray antennas," in *Proc. IEEE 13th Eur. Conf. Antennas Propag. (EuCAP)*, Krakow, Poland, 2019, pp. 1–4.

[37] M. Mussetta, W. Zhang, A. Wang, H. Chen, and R. Zich, "Frequency response optimization of a double layer reflectarray antenna," in *Proc. IEEE Antennas Propag. Soc. Int. Symp.*, Honolulu, HI, USA, 2007, pp. 5319–5322.

[38] P. Nayeri, A. Z. Elsherbeni, and F. Yang, "Radiation analysis approaches for reflectarray antennas [antenna designer's notebook]," *IEEE Antennas Propag. Mag.*, vol. 55, no. 1, pp. 127–134, Feb. 2013.

[39] A. Niccolai, F. Grimaccia, M. Mussetta, and R. Zich, "Optimal task allocation in wireless sensor networks by means of social network optimization," *Mathematics*, vol. 7, no. 4, p. 315, 2019.

[40] S. K. Goudos, Z. D. Zaharis, and K. B. Baltzis, "Particle swarm optimization as applied to electromagnetic design problems," *Int. J. Swarm Intell. Res.*, vol. 9, no. 2, pp. 47–82, 2018.

[41] H. Ma, D. Simon, P. Siarry, Z. Yang, and M. Fei, "Biogeography-based optimization: A 10-year review," *IEEE Trans. Emerg. Topics Comput. Intell.*, vol. 1, no. 5, pp. 391–407, Oct. 2017.

[42] P. Pirinoli, A. Massaccesi, and M. Beccaria, "Application of the M_m C_n-BBO algorithms to the optimization of antenna problems," in *Proc. IEEE Int. Conf. Electromagn. Adv. Appl. (ICEAA)*, Verona, Italy, 2017, pp. 1850–1854.

[43] W. Khatib and P. J. Fleming, "The stud GA: A mini revolution?" in *Proc. Int. Conf. Parallel Problem Solving Nat.*, 1998, pp. 683–691.

[44] D. W. Zimmerman and B. D. Zumbo, "Relative power of the wilcoxon test, the friedman test, and repeated-measures anova on ranks," *J. Exp. Educ.*, vol. 62, no. 1, pp. 75–86, 1993.

[45] S. V. Hum, M. Okoniewski, and R. J. Davies, "Modeling and design of electronically tunable reflectarrays," *IEEE Trans. Antennas Propag.*, vol. 55, no. 8, pp. 2200–2210, Aug. 2007.

[46] M. Riel and J.-J. Laurin, "Design of an electronically beam scanning reflectarray using aperture-coupled elements," *IEEE Trans. Antennas Propag.*, vol. 55, no. 5, pp. 1260–1266, May 2007.

[47] E. Carrasco, M. Barba, and J. A. Encinar, "X-band reflectarray antenna with switching-beam using PIN diodes and gathered elements," *IEEE Trans. Antennas Propag.*, vol. 60, no. 12, pp. 5700–5708, Dec. 2012.

[48] W. Hu *et al.*, "Design and measurement of reconfigurable millimeter wave reflectarray cells with nematic liquid crystal," *IEEE Trans. Antennas Propag.*, vol. 56, no. 10, pp. 3112–3117, Oct. 2008.

[49] O. Bayraktar, O. A. Civi, and T. Akin, "Beam switching reflectarray monolithically integrated with RF MEMS switches," *IEEE Trans. Antennas Propag.*, vol. 60, no. 2, pp. 854–862, Feb. 2012.

[50] P. Nayeri, F. Yang, and A. Z. Elsherbeni, "Beam-scanning reflectarray antennas: A technical overview and state of the art," *IEEE Antennas Propag. Mag.*, vol. 57, no. 4, pp. 32–47, Aug. 2015.

[51] G.-B. Wu, S.-W. Qu, and S. Yang, "Wide-angle beam-scanning reflectarray with mechanical steering," *IEEE Trans. Antennas Propag.*, vol. 66, no. 1, pp. 172–181, Jan. 2018.

[52] X. Yang *et al.*, "A mechanically reconfigurable reflectarray with slotted patches of tunable height," *IEEE Antennas Wireless Propag. Lett.*, vol. 17, pp. 555–558, 2018.

[53] P. Mei, S. Zhang, and G. F. Pedersen, "A low-cost, high-efficiency and full-metal reflectarray antenna with mechanically 2-D beam-steerable capabilities for 5G applications," *IEEE Trans. Antennas Propag.*, early access, May 14, 2020, doi: 10.1109/TAP.2020.2993077.

[54] G.-B. Wu, S.-W. Qu, S. Yang, and C. H. Chan, "Low-cost 1-D beam-steering reflectarray with±70 scan coverage," *IEEE Trans. Antennas Propag.*, vol. 68, no. 6, pp. 5009–5014, Jun. 2020.

[55] M. Beccaria *et al.*, "Feed system optimization for convex conformal reflectarray antennas," in *Proc. IEEE Int. Symp. Antennas Propag. USNC/URSI Nat. Radio Sci. Meeting*, San Diego, CA, USA, 2017, pp. 1187–1188.

[56] O. Dursun, B. Ekici, and S. Sarıyıldız, "Time-cost optimization at the conceptual design stage using differential evolution: Case of single family housing projects in Germany," in *Proc. IEEE Congr. Evol. Comput. (CEC)*, Sendai, Japan, 2015, pp. 2237–2244.

[57] *MATLAB: Parallel Computing Toolbox*, MathWorks, Natick, MA, USA. Accessed: Sep. 25, 2020. [Online]. Available: https://it.mathworks.com/products/parallel-computing.html

ALESSANDRO NICCOLAI (Member, IEEE) received the bachelor's degree, and the master's degree (*cum laude*) in mechanical engineering, and the Ph.D. degree (*cum laude*) in electrical engineering from the Politecnico di Milano in 2014, 2016, and 2019, respectively. He did an advanced study program, named Alta Scuola Politecnica, with the Politecnico di Milano and Politecnico di Torino and received the double degree in mechanical engineering from Politecnico di Torino. He is currently a Postdoctoral Researcher with the Politecnico di Milano. He has published more than 45 papers in international journals or conferences. His main research activities concern computational intelligence, particularly focused on evolutionary optimization algorithms and neural networks.

MICHELE BECCARIA (Member, IEEE) was born in Enna, Italy, on July 24, 1991. He received the B.Sc, the M.Sc. degree, and the Ph.D. degree (*cum laude*) in applied electromagnetics from the Politecnico di Torino in 2013, 2015, and 2019, respectively. He has been a Research Fellow with the Department of Electronics and Telecommunications, Politecnico di Torino, Turin, since January 2019. In 2017 and 2018, he was a visiting Ph.D. student with Tsinghua University, Beijing, China, under the supervision of Prof. Fan Yang. His research interests include reflectarray antennas, transmitarray antennas and the application of new optimization algorithms for complex antenna design. He was also recognized as the winner of two grants for attending the Ph.D. courses of ESoA in 2016 and in 2018 as one of the Best Ph.D. Students at Politecnico di Torino with the Ph.D. Quality Award. He was included in the Technical Committee of Conference of International Relevance (ICCE 2018, 2020) and serves many journals of the IET group as a reviewer. In 2020, he received the 2019 IEEE AP/ED/MTT North Italy Chapter Thesis Awards with the Best Ph.D. Thesis Antennas and Propagation Society for the thesis "Design of Innovative Reflectarray and Transmitarray Antennas."

RICCARDO E. ZICH (Member, IEEE) was born in Torino, Italy, in May 25, 1966. He received the Laurea (M.S.) (*summa cum laude*) and Ph.D. degrees in electronic engineering from the Politecnico di Torino, in 1989 and 1993, respectively. In 1991, he joined the Politecnico di Torino as an Assistant Professor of electrical engineering. He joined the Politecnico di Milano as an Associate Professor of electrical engineering in 1998 and became a Full Professor in 2002. He has authored or coauthored more than 230 international papers and chaired or organized more than 30 special sessions in International Symposia. His main research activities concern analytical and numerical techniques in high- and low-frequency electromagnetics, electromagnetic compatibility, evolutionary computation and nonconventional antennas, and wireless sensor networks designs. He is a member of the IEEE Antennas and Propagation Society, the IEEE Electromagnetic Compatibility Society, the IEEE Microwave Theory and Techniques Society, the IEEE Circuits and Systems Society, the International Union of Radio Science, and the Institute of Electronics, Information, and Communication Engineers.

ANDREA MASSACCESI (Member, IEEE) was born in Osimo, Italy, in 1987. He received the B.S. degree in electronic engineering from the Université Politecnica delle Marche, Ancona, Italy, in 2012, the M.S. degree in electronic engineering and the Ph.D. degree (*cum laude*) in electrical, electronic and communication engineering from the Politecnico di Torino, Turin, Italy, in 2015 and 2019, respectively. From November 2017 to May 2018, he was a visiting Ph.D. student with Loughborough University, Loughborough, U.K., within the Symeta research program. Since January 2020, he has been a Research Fellow with the Department of Electronics and Telecommunications, Politecnico di Torino, Turin, Italy. His research activities include the study of underwater electromagnetic propagation and the design of proper antennas for underwater environments, the design and manufacturing of innovative transmitarray and reflectarray antennas exploiting 3D-printing techniques, and the development of efficient global optimization techniques suitable for electromagnetic problems.

PAOLA PIRINOLI (Member, IEEE) received the M.S. (Laurea) and Ph.D. (Dottorato di Ricerca) degrees in electronic engineering from the Politecnico di Torino, Italy, in 1989 and 1993, respectively. From 1994 to 2003, she was an Assistant Professor (Ricercatore) of electromagnetic fields with the Department of Electronics and Telecommunications, Politecnico di Torino, where she was an Associate Professor from 2003 to 2018, and has been a Full Professor since 2018. From 1996 to 1997, she was a Visiting Research Fellow with the University of Nice, Sophia Antipolis, France. In 2014, 2015, and 2017, she was a Visiting Research Fellow with Tsinghua University, Beijing, China. She has coauthored around 250 journal articles and conference papers. Her main research activities include the development of analytically based numerical techniques, essentially devoted to the fast and accurate analysis of printed structures on planar or curved substrates, the modeling of nonconventional substrates, as chiral and anisotropic ones, the development of innovative and efficient global optimization techniques, and the design of innovative reflectarray and transmitarray antennas. In 1998, she received the URSI Young Scientist Award and the Barzilai Prize for the Best Paper at the National Italian Congress of Electromagnetic (XII RiNEm). In 2000, she was the recipient of the Prize for the Best Oral Paper on Antennas at the Millennium Conference on Antennas and Propagation. She serves as a reviewer for several international journals and conferences. She is a member of the TPC and the organizing committee of several international conferences.